Inorg. Chem. **2005**, *44*, 6529–6535

Tris(pyronato)- and Tris(pyridonato)-ruthenium(III) Complexes and Solution NMR Studies

David C. Kennedy, Adam Wu, Brian O. Patrick, and Brian R. James*

Department of Chemistry, The University of British Columbia, Vancouver, British Columbia, Canada V6T 1Z1

Received January 10, 2005

The water-soluble Ru^{III} maltolato, ethylmaltolato, and pyridonato complexes, $Ru(O–O')_3$ (O–O′ = ma (**1a**), etma (**1b**), pyd (**2a**)), were synthesized (Hma = 3-hydroxy-2-methyl-4-pyrone, Hetma = 2-ethyl-3-hydroxy-4-pyrone, Hpyd = 3-hydroxy-1,2-dimethyl-4-pyridone). The complexes were characterized by elemental analysis, NMR and IR spectroscopies, MS, solution conductivity, and cyclic voltammetry, and in the case of $Ru(ma)_3$, by X-ray crystallography, which revealed a mer configuration. The paramagnetic ^{1}H NMR resonances of **1a**, **1b**, and **2a** were assigned using 2D methods (^{1}H COSY and ^{1}H-^{13}C HMQC) and variable-temperature ^{1}H NMR data and showed that **1a** and **1b** exist in aqueous solution predominantly as a mer isomer, while **2a** is a mixture of mer and fac isomers. Although a ^{13}C NMR spectrum could not be measured directly for **1a**, a partial ^{13}C spectrum was generated from the ^{1}H-^{13}C HMQC spectrum. Complexes **1a** and **1b** were tested for anti-proliferatory activity against the human breast cancer cell line MDA-MB-435S and gave IC_{50} values of 140 and 90 μM, respectively.

Introduction

Greaves and Griffith first prepared the tris(maltolato)-ruthenium(III) complex, $Ru(ma)_3$, in 1988, but no NMR spectroscopic or X-ray structural data were given to establish its configuration (Hma = 3-hydroxy-2-methyl-4-pyrone, Chart 1).[1] Several Ru complexes containing an ancillary ma, etma (Hetma = 2-ethyl-3-hydroxy-4-pyrone), or the related pyd ligand (Hpyd = 3-hydroxy-1,2-dimethyl-4-pyridone, Chart 1) have been reported since, for both Ru(III)[2] [$RuCl_2(PPh_3)_2$(ma), $RuCl_2(PPh_3)_2$(pyd), and $RuBr_2(AsPh_3)_2$(pyd)] and Ru(II) [$RuH(PPh_3)_3$(ma),[2] $RuH(PPh_3)_3$(pyd),[2] RuCl(mes)-(O−O′), where mes = 1,3,5-trimethylbenzene and O−O′ = ma, pyd, or etma,[3,4] RuCl(*p*-cymene)(pyd),[5] and $Ru(ma)_2(L)_2$, where L = DMSO, COD, or PPh_3];[6] the last paper reported crystal structures for the *cis*-DMSO and COD complexes.

Recently, we have expanded the syntheses of Ru^{II} maltolato−sulfoxide complexes to include $Ru(O–O')_2(L)_2$ (O−O′ = ma, etma; L = DMSO, tetramethylenesulfoxide, $(L)_2$ = 1,2-bis(ethylsulfinyl)ethane), and examined their in vitro anti-proliferatory activity against a human breast cancer cell line using a so-called MTT assay.[7] The anti-cancer activity of Ru−sulfoxide complexes is a topic of intense current interest,[7] and the incorporation of maltol (a well-known, nontoxic food additive)[8] endows the complex with water-solubility. This, coupled with the frequently proposed use of Ru(III) as pro-drugs, as the precursors for the possibly more active Ru(II) species,[7] led us to initiate studies on Ru-(III)−maltol chemistry, and this paper describes the synthesis and characterization of water-soluble Ru^{III} maltolato, ethylmaltolato, and pyridonato complexes, $Ru(O–O')_3$ (O−O′ = ma (**1a**), etma (**1b**), and pyd (**2a**), Chart 2), with the solution structures fully characterized by one- and two-dimensional NMR spectroscopic techniques. X-ray crystallography reveals the mer configuration for the solid-state structure of **1a**. The ^{1}H NMR studies on these paramagnetic species are consid-

Chart 1

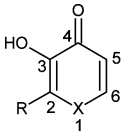

R = Me, X = O, 3-hydroxy-2-methyl-4-pyrone (Hma);
R = Et, X = O, 2-ethyl-3-hydroxy-4-pyrone (Hetma);
R = Me, X = NMe, 3-hydroxy-1,2-dimethyl-4-pyridone (Hpyd)

* To whom correspondence should be addressed. E-mail: brj@chem.ubc.ca.

(1) Greaves, S. J.; Griffith, W. P. *Polyhedron* **1988**, *7*, 1973.
(2) El-Hendawy, A. M. *Transition Met. Chem.* **1992**, *17*, 250.
(3) Carter, L.; Davies, D. L.; Fawcett, J.; Russell, D. R. *Polyhedron* **1993**, *12*, 1599.
(4) Capper, G.; Carter, L. C.; Davies, D. L.; Fawcett, J.; Russell, D. R. *J. Chem. Soc., Dalton Trans.* **1996**, 1399.
(5) Lang, R.; Polborn, K.; Severin, T.; Severin, K. *Inorg. Chim. Acta* **1999**, *294*, 62.
(6) Fryzuk, M. D.; Jonker, M. J.; Rettig, S. J. *Chem. Commun.* **1997**, 377.
(7) Wu, A.; Kennedy, D. C.; Patrick, B. O.; James, B. R. *Inorg. Chem.* **2003**, *42*, 7579 and references therein.
(8) Sun, Y.; James, B. R.; Rettig, S. J.; Orvig, C. *Inorg. Chem.* **1996**, *35*, 1667.

10.1021/ic050034d CCC: $30.25
Published on Web 08/13/2005

Chart 2

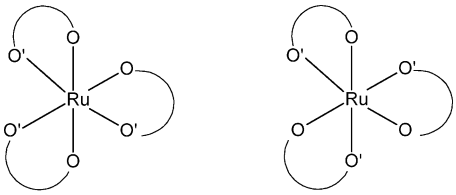

mer-Ru(O-O')$_3$ *fac*-Ru(O-O')$_3$

ered particularly significant, as the data present the first assignments of the various resonances of the maltolato and related pyridonate ligands coordinated at Ru(III). Data from the testing of **1a** and **1b** against human breast cancer cells by the MTT assay show that these complexes exhibit significant anti-proliferatory activity.

Experimental Section

Materials for Synthesis. Reagent grade solvents (Fisher Scientific) were dried before use, using standard procedures[9] under N_2, and the deuterated solvents (Cambridge Isotope Laboratories) were used as received. $RuCl_3 \cdot 3H_2O$ (Colonial Metals), maltol (Cultor Food Science), ethylmaltol (Pfizer Food Science), NaOAc (Fisher), NaOMe (Fisher), H(pyd) (Aldrich), and silica gel (230−400 mesh from SiliCycle) were used as received. Standard Schlenk techniques were used for synthesis of the complexes.

Physical Techniques and Instrumentation. ^{1}H NMR, ^{1}H COSY, and ^{1}H-^{13}C HMQC spectra were recorded at room temperature (∼20 °C), unless stated otherwise, on a Bruker AV300 instrument, with the chemical shifts calibrated using the residual proton resonances from the deuterated solvents; the resonances for the paramagnetic species were all singlets of varying widths. Elemental analyses were performed on a Carlo Erba EA 1108 CHN−O analyzer, and mass spectral data (reported as *m*/*z* values) were acquired on a Kratos Concept IIHQ LSIMS instrument using a thioglycerol matrix or on a Bruker Esquire ES spectrometer by the staff of this department (c/o Dr. Y. Ling). UV−vis spectra were recorded at room temperature on a Hewlett-Packard 8452A diode-array spectrometer, and data are presented as λ_{max} in nm ($\epsilon_{max} \times 10^{-3}$ M^{-1} cm^{-1}). IR spectra (KBr pellet) were recorded on a Bomem−Michelson MB-100 FT-IR spectrometer, and selected more intense bands are given as ν values (cm^{-1}).[10] Conductivity measurements, carried out on a RCM151B Serfass conductance bridge (A. H. Thomas Co. Ltd.) with a 3403 cell (Yellow Springs Instrument Company), were calibrated using a 0.01000 M aqueous KCl solution ($\Lambda_M = 141.3$ Ω^{-1} cm^2 mol^{-1} at 25 °C, cell constant = 1.016 cm^{-1}, data are given in units of Ω^{-1} cm^2 mol^{-1}).[11,12] CV was performed in MeCN or CH_2Cl_2 containing 0.1 M [^{n}Bu$_4$N]PF_6 as supporting electrolyte. Voltammograms were recorded on a Pine Bipotentiostat (Model AFCBP1) with PineChem, version 2.00, software; the scan-rate was 100 mV s^{-1} using a Pt working electrode, a Pt wire counter electrode, and a Ag wire reference electrode, with $FeCp_2$ (0.40 V vs SCE) and $FeCp^*_2$ (−0.08 V vs SCE) as internal calibrants.[13] $E_{1/2}$ values are given in V vs SCE. Atomic Absorption Spectroscopy (AAS) was performed on a Varian SpectrAA-300 Zeeman instrument that was calibrated using stock solutions of Ru (obtained from Aldrich), and a Ru hollow-cathode lamp at a 10 mA current (λ_{max} = 349.9 nm).

Table 1. Crystallographic Data for **1a**

formula	$C_{18}H_{15}O_9Ru$
fw	476.37
cryst color, habit	red, prism
cryst size (mm)	0.30 × 0.20 × 0.10
space group	*Pbca*
a (Å)	17.017(3)
b (Å)	11.6860(8)
c (Å)	18.6414(14)
β (deg)	90
V (Å^3)	3707.0(7)
Z	8
μ (mm^{-1})	0.895
D_{calc} (g cm^{-3})	1.707
total reflns	10999
unique reflns	3820
R_{int}	0.086
no. variables	241
R1 ($I > 2\sigma(I)$)	0.0450 (1991 obs. refl.)
wR2[a]	0.1060 (all data)
GOF	0.820

[a] $w = 1/[\sigma^2(F_o^2) + (0.0000P)^2 + 0.0000P]$, where $P = (F_o^2 + 2F_c^2)/3$.

X-ray Crystallography. Measurements were made at 173(1) K on a Rigaku/ADSC CCD area detector with graphite monochromated Mo Kα radiation (0.71069 Å). Some crystallographic data for **1a** are shown in Table 1. The final unit-cell parameters were based on 3820 reflections. The data for **1a** were collected and processed using the d*TREK program.[14] The structure revealed the presence of the mer isomer; the molecule defined by the list of refined coordinates is the Λ form, but the *Pbca* centric space group requires that the unit cell contains equal amounts of the Λ and Δ forms. The structure shows 2-fold disorder for one of the ligands, in which the Me group site (C18) is occupied ∼50% of the time by the molecule oriented, as in the left part of Figure 1, and ∼50% of the time by the same molecule in the orientation shown on the right-hand side; the two orientations are related by a 180° rotation about an axis through the Ru atom and the middle of the C15−O9 bond of the disordered bond. Both fragments were modeled using constraints on both bond lengths and angles, in such a way that the geometry of the ligand would be similar to that of the two nondisordered ligands but would not unduly influence the Ru−O bond distances. The structure was solved using direct methods,[15] and both fragments were refined isotropically, while all non-hydrogen atoms were refined anisotropically.

MTT Assay. Leibovitz's L-15 medium with L-glutamine (L-15), fetal bovine serum (FBS), zinc bovine insulin, phosphate-buffered saline solution 7.4 (PBS), and trypsin-EDTA (0.25% trypsin in 1 mM Na_4(EDTA)) were purchased from Gibco. Ninety-six-well plates and T-25 and T-75 flasks were purchased from Falcon. MTT was purchased from Aldrich. The growth medium for the MDA-MB-435S breast cell line, purchased from American Type Culture Collection (ATCC), consisted of 500 mL L-15, 50 mL FBS, and 5.0 mg of insulin. PBS, MTT, and the growth medium were stored at 4 °C, while the trypsin-EDTA and FBS were stored at −20 °C. FBS was filter-sterilized through 0.1 μm filters before use. We recently published procedural details for the MTT assay.[7]

Ru Uptake by Cells. A suspension of MDA-MB-435S cells (1 × 10^6 in 1 mL of media) was added to solutions of **1a** and **1b** in

(9) Gordon, A. J.; Ford, R. A. *The Chemist's Companion: A Handbook of Practical Data, Techniques, and References*; John Wiley & Sons: New York, 1972.
(10) Pavia, D. L.; Lampman, G. M.; Kriz, G. S. *Introduction to Spectroscopy*, 2nd ed.; Harcourt Brace: Orlando, FL, 1996.
(11) Geary, W. J. *Coord. Chem. Rev.* **1971**, *7*, 81.
(12) Huheey, J. E. *Inorganic Chemistry: Principles of Structure and Reactivity*, 3rd ed.; Harper Collins: New York, 1983.
(13) Connelly, N. G.; Geiger, W. E. *Chem. Rev.* **1996**, *96*, 877.
(14) *d*TREK, Area Detector Software*, version 7.11; Molecular Structure Corporation: The Woodlands,TX, **2001**.
(15) *SIR92*; Altomare, A.; Cascarano, M.; Giacovazzo, C.; Guagliardi, A. *J. Appl. Crystallogr.* **1994**, *26*, 343.

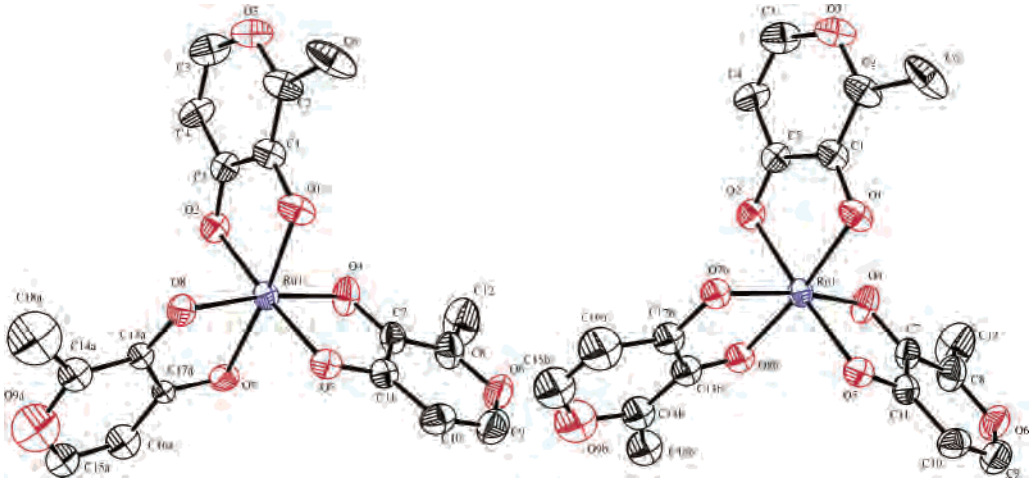

Figure 1. ORTEP diagrams of the Λ isomer of *mer*-Ru(ma)$_3$ (**1a**) with 50% probability thermal ellipsoids. Two-fold disorder in one ligand gives rise to ~50% occupancy by the two orientations shown (see text).

PBS (9 mL), giving a final complex concentration of 100 μM and a final volume of 10 mL. The mixture was incubated at 37 °C and shaken (150 rpm) for 3 h, and then it was centrifuged (10 min at 800 rpm). The resulting pellet was washed twice with PBS (5 mL), dried (16 h at 37 °C), and then dissolved in concentrated HNO_3 (100 μL), followed by dilution to 250 μL with doubly distilled H_2O prior to analysis by AAS.

***mer*-Ru(ma)$_3$ (1a).** This complex was synthesized by a literature procedure[1] with additional workup steps. Maltol (2.50 g, 19.2 mmol) was added, under N_2, to a brown aqueous (80 mL) solution of $RuCl_3 \cdot 3H_2O$ (1.01 g, 3.86 mmol) and NaOAc (4.0 g, 30 mmol), and the mixture was refluxed for 6 h. The resulting red precipitate was collected and dissolved in CH_2Cl_2 (40 mL); the solution was filtered through Celite (2 g) to remove a black impurity. The filtrate was reduced in volume to ~5 mL, and then hexane (30 mL) was added to precipitate the red solid, which was collected and dried in vacuo at 78 °C for 48 h. Yield: 0.95 g (52%). Anal. Calcd for $C_{18}H_{15}O_9Ru$: C, 45.38; H, 3.17. Found: C, 45.32; H, 3.19. ^{1}H NMR (CD_2Cl_2): δ 43.17, 41.03, 21.11 (CH_3), 11.84 (H_5-ma), 9.20 (H_6-ma), 3.43 (H_6-ma), −4.61 (H_5-ma), 0.92 (H_6-ma), −0.87 (H_5-ma). IR: ν 1600, 1551, 1466, 1261, 1199. LR-MS (+LSIMS): 477 (M^+), 352 (M^+ − ma). UV−vis (H_2O): 216 (45.4), 284 (14.1), 380 (10.2). CV (MeCN): $E_{1/2}(Ru^{III/II}) = -1.13$ V, $E_{1/2}(Ru^{IV/III}) =$ 0.52 V vs SCE. CV (CH_2Cl_2): $E_{1/2}(Ru^{III/II}) = -1.27$ V, $E_{1/2}(Ru^{IV/III})$ = 0.48 V vs SCE. Λ_M: 2 (CH_2Cl_2), 25 (H_2O). The IR data and CV data in CH_2Cl_2 agree with the literature values.[1]

***mer*-Ru(etma)$_3$ (1b).** The complex was synthesized in a manner similar to that for **1a**, except ethylmaltol (2.80 g, 20 mmol) was used. Yield: 0.83 g (45%). Anal. Calcd for $C_{21}H_{21}O_9Ru$: C, 48.65; H, 4.08. Found: C, 48.64; H, 4.09. ^{1}H NMR (CD_2Cl_2): δ 40.10, 35.32, 38.80, 33.41, 21.72, 18.88 (CH_2CH$_3$), 4.86, 4.78, 2.05 (CH$_2$CH_3), 12.54 (H_5-ema), 9.02 (H_6-ema), 4.86 (H_6-ema), −4.91 (H_5-ema), 1.20 (H_6-ema), −0.79 (H_5-ema). IR: ν 1596, 1550, 1471, 1258, 1187. LR-MS (+LSIMS): 519 (M^+), 380 (M^+ − ema). UV−vis (H_2O): 216 (45.1), 284 (14.4), 382 (10.6). CV (MeCN): $E_{1/2}(Ru^{III/II}) = -1.14$ V, $E_{1/2}(Ru^{IV/III}) = 0.52$ V vs SCE. CV (CH_2Cl_2): $E_{1/2}(Ru^{III/II}) = -1.29$ V, $E_{1/2}(Ru^{IV/III}) = 0.49$ V vs SCE. Λ_M: 5 (CH_2Cl_2), 36 (H_2O).

Ru(pyd)$_3$ (2a). A suspension of $RuCl_3 \cdot 3H_2O$ (100 mg, 0.382 mmol), NaOMe (207 mg, 3.83 mmol), and H(pyd) (266 mg, 1.91 mmol) in EtOH (20 mL) was refluxed in air for 3 h to give a dark red solution. The solvent was removed under vacuum; the residue was extracted with CH_2Cl_2 (20 mL), and the mixture was filtered through Celite. The filtrate solvent was then removed under vacuum, and the residue, dissolved in CH_2Cl_2:MeOH (1:1), was loaded onto a silica gel column (2 cm × 8 cm) and eluted with the same solvent combination. The red fraction was collected and evaporated to dryness under vacuum. The residue was dissolved in CH_2Cl_2 and reprecipitated by the addition of hexanes; the dark orange-red solid was collected and dried in vacuo at 78 °C. Complex **2a** is hygroscopic and is, therefore, stored under vacuum. Yield: 122 mg (62%). Anal. Calcd for $C_{21}H_{24}O_6N_3Ru \cdot H_2O$: C, 47.28; H, 4.91; N, 7.88. Found: C, 47.18; H, 5.16; N, 8.04. ^{1}H NMR (CD_2Cl_2): δ 30.39, 27.80, 22.71 (*mer*-CCH_3), 7.89, 7.00, 5.71 (*mer*-NCH_3), 8.59 (*mer*-*H*(5)), 6.03 (*mer*-*H*(6)), −1.13 (*mer*-*H*(6)), −1.54 (*mer*-*H*(5)), 0.27 (*mer*-*H*(6)), −4.26 (*mer*-*H*(5)), 22.86 (*fac*-CCH_3), 10.44 (*fac*-NCH_3), 7.37 (*fac*-*H*(6)), 2.89 (*fac*-*H*(5)). LR-MS (+ESI, MeOH/CH_2Cl_2 (1:1)): 516 (M^+). IR: ν 1600, 1542, 1498. CV (CH_2Cl_2): $E_{1/2}(Ru^{III/II}) = -1.66$, $E_{1/2}(Ru^{IV/III}) = -0.07$, $E_{1/2}(Ru^{V/IV}) = 1.18$ V vs SCE. Λ_M: 0 (CH_2Cl_2), 4 (H_2O).

Table 2. Selected Bond Distances and Angles for **1a** with Estimated Standard Deviations in Parentheses

bond	length (Å)	bond	angle (°)
Ru(1)−O(1) (hydroxy)	1.993(3)	O(1)−Ru(1)−O(2)	82.76(14)
Ru(1)−O(2) (keto)	2.050(4)	O(4)−Ru(1)−O(5)	82.65(15)
Ru(1)−O(4) (hydroxy)	1.991(4)	O(7)−Ru(1)−O(8)	83.41(19)
Ru(1)−O(5) (keto)	2.055(3)	O(7b)−Ru(1)−O(8b)	79.3(4)
Ru(1)−O(7) (keto)	2.081(6)	O(1)−Ru(1)−O(4)	93.51(18)
Ru(1)−O(8) (hydroxy)	2.070(5)	O(1)−Ru(1)−O(5)	94.51(14)
Ru(1)−O(7b) (keto)	2.066(10)	O(1)−Ru(1)−O(7)	173.33(19)
Ru(1)−O(8b) (hydroxy)	1.984(11)	O(4)−Ru(1)−O(7b)	168.6(3)

Results and Discussion

Complexes Ru(ma)$_3$ (**1a**) and Ru(etma)$_3$ (**1b**) were synthesized by refluxing an aqueous solution of $RuCl_3 \cdot 3H_2O$, NaOAc, and maltol or ethylmaltol, respectively, according to a literature procedure,[1] although we used additional workup procedures involving CH_2Cl_2 extraction, filtration through Celite, and precipitation with hexanes. Crystals of **1a**, grown by slow evaporation of an acetone solution of the complex, were analyzed by X-ray diffraction which revealed a mer configuration with respect to the corresponding O atoms (Chart 2); the measured structure showed a 2-fold disorder in one of the ligands, the modeling revealing ~50% occupancy by the orientations illustrated in Figure 1. Table 2 shows selected bond distances and angles. The somewhat distorted octahedral coordination environment

Table 3. Variable-Temperature Chemical Shifts of **1a** (300 MHz, CD_2Cl_2) Including Values at $T = \infty$, as Determined by Linear Regression

temp (K)	δ Me1	δ Me2	δ Me3	δ $H_a(5)$	δ $H_a(6)$	δ $H_b(6)$	δ $H_c(6)$	δ $H_c(5)$	δ $H_b(5)$
∞	9.0	10.0	14.3	4.9	8.0	9.0	9.0	7.5	6.7
295	43.17	41.03	21.11	11.84	9.20	3.43	0.92	−0.87	−4.61
280	45.97	43.04	22.06	12.66	8.87	3.26	0.09	−1.37	−5.02
267	47.52	44.15	22.39	12.96	8.89	3.01	−0.33	−1.72	−5.49
256	49.16	45.94	22.81	13.27	8.93	2.72	−0.76	−2.08	−5.99
244	50.97	47.61	23.26	13.63	8.97	2.39	−1.22	−2.49	−6.55
233	52.99	49.38	23.72	14.02	9.00	2.04	−1.72	−2.93	−7.15
221	55.16	51.48	24.23	14.47	9.04	1.65	−2.31	−3.44	−7.84
212	57.62	53.68	24.81	14.98	9.09	1.22	−2.95	−3.99	−8.57
200	60.35	56.06	25.38	15.52	9.13	0.70	−3.66	−4.63	−9.39

shows the bite angles of the ligands within the five-membered rings of between 79.3 and 83.41° (Table 2).

The mer configuration has also been observed for Fe(ma)$_3$ [16] and Al(ma)$_3$ [17] (complexes of interest in iron-deficiency anemia and neurology, respectively), and the 2-fold disorder seen in **1a** was also observed in the structure of *mer*-Al(ma)$_3$. In Fe(ma)$_3$, the unit cell of which contained four discrete mer isomers, two with the Λ configuration and two with the Δ configuration, a significant difference in the average Fe−O bond length was observed between the Fe−O (keto) (2.065 Å) and Fe−O (hydroxy) (1.987 Å) bonds. Similarly, the average Ru−O bond length for the Ru−O (keto) groups (2.063 Å) is longer than that observed for the Ru−O (hydroxy) groups (2.009 Å, Table 2).

The ^{1}H COSY spectrum of Ru(ma)$_3$ (**1a**) in CD_2Cl_2 (Figure 2) shows three resonance coupling pairs at δ −4.61 *H*(5), 3.43 *H*(6), −0.87 *H*(5), 0.92 *H*(6); and 9.20 *H*(6), 11.84 (*H*(5)); each pair is assigned to one set of the ma *H*(5)/*H*(6) protons. The resonances were assigned to either *H*(5) or *H*(6) by plotting 1/*T* vs chemical shift for each resonance as determined by low-temperature ^{1}H NMR experiments (Table 3 and Figure 3). Although such plots are not necessarily linear as 1/*T* approaches zero, the intercepts at 1/*T* = 0 from linear plots are often used to estimate the values expected for a corresponding diamagnetic species.[18] For each pair of singlets observed in the ^{1}H-^{1}H COSY spectrum of **1a**, one can be assigned as *H*(5) and the other as *H*(6). $H_a(5)$ and $H_a(6)$ show correlation in Figure 2 and, in Figure 3, give intercepts on the *x* axis at δ ~5 and ~8, respectively. From these values, $H_a(5)$ is thus assigned as an *H*(5) proton and $H_a(6)$ as an *H*(6) proton. Similarly, $H_b(6)$ and $H_c(6)$ are assigned as *H*(6) protons, and $H_b(5)$ and $H_c(5)$ are assigned as *H*(5) protons. We are confident of the assignments because (i) the extrapolated values ($T = \infty$ in Table 3) in every case are within 1.5 ppm of the diamagnetic values measured for free maltol in CD_2Cl_2 (*H*(5) at δ 6.4, and *H*(6) at δ 7.7) and (ii) the magnitude of the hyperfine shift for *H*(5) is always greater than that for *H*(6) as expected because *H*(5) is closer to the Ru(III) center. The three downfield shifted resonances assigned to the Me groups resulted in no cross-peaks in the ^{1}H COSY spectrum, as expected. The *x* intercepts for the resonances of these groups from the low-temperature ^{1}H NMR data (δ 14.3, 10.0 and 9.0, Table 3) do not, however, correlate well with the Me resonance of free maltol (δ 2.4).

The ^{1}H NMR data suggest that the mer geometry for **1a**

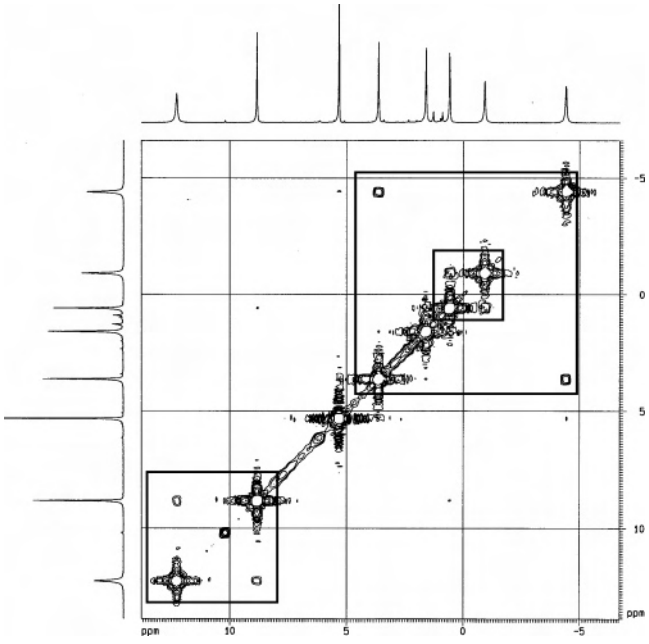

Figure 2. ^{1}H COSY NMR spectrum (300 MHz, CD_2Cl_2) of **1a**. The squares indicate ma *H*(5)/*H*(6) coupling pairs.

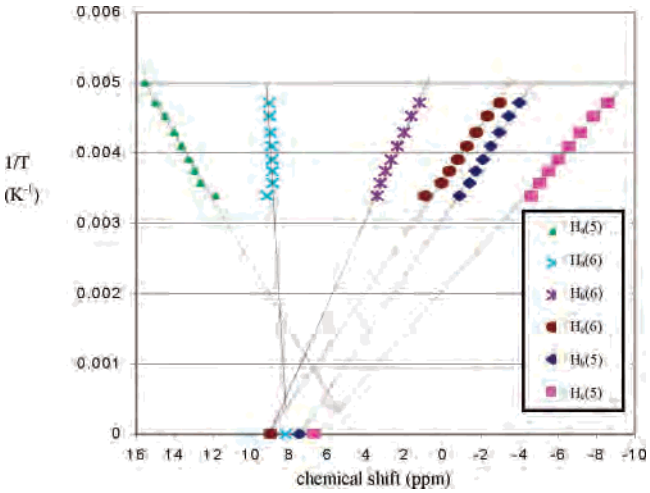

Figure 3. Plot of 1/*T* (K^{-1}) vs the chemical shift (ppm) from 200 to 295 K for the *H*(5) and *H*(6) protons on each ma ring of Ru(ma)$_3$ (**1a**).

(16) Ahmet, M. T.; Frampton, C. S.; Silver, J. *J. Chem. Soc., Dalton Trans.* **1988**, 1159.
(17) Finnegan, M. M.; Rettig, S. J.; Orvig, C. *J. Am. Chem. Soc.* **1986**, *108*, 5033.
(18) Banci, L.; Bertini, I.; Luchinat, C.; Pierattelli, R.; Shokhirev, N. V.; Walker, F. A. *J. Am. Chem. Soc.* **1998**, *120*, 8472.

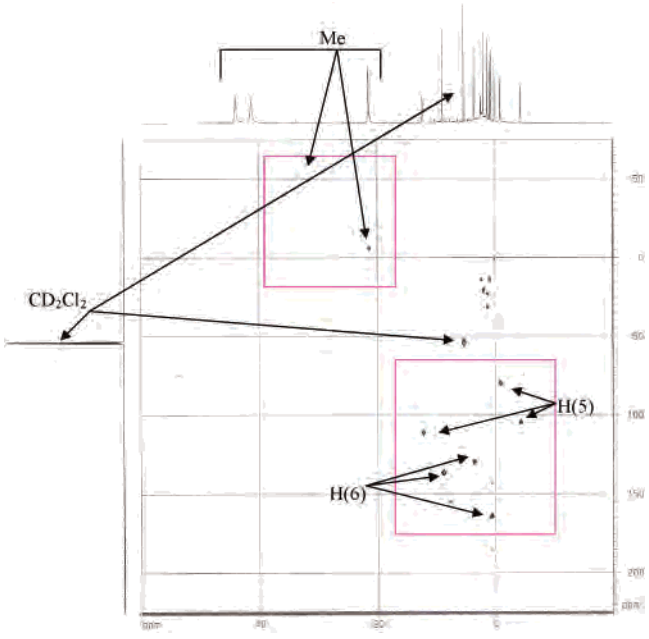

Figure 4. ^{1}H-^{13}C HMQC spectrum (300 MHz, CD_2Cl_2) of Ru(ma)$_3$ (**1a**) with the ^{13}C spectrum on the left-hand side and the ^{1}H spectrum at the top (some decomposition occurred during acquisition of the spectrum, leading to additional cross-peaks). The cross-peaks for the *H*(5) and *H*(6) protons, the solvent, and two Me groups are indicated with arrows.

is retained in CD_2Cl_2 solution, although a trace amount of the fac isomer is also present as indicated by a singlet resonance at δ 33.71 for the C*H*$_3$ group of this isomer. The ^{1}H-^{13}C HMQC spectrum (Figure 4) provides further evidence for the ^{1}H assignments, as the six maltolato ring proton signals each have a cross-peak between δ 75 and 175 in the ^{13}C NMR spectrum as expected for protons on an sp^2-hybridized carbon.[10] Two cross-peaks for Me groups are also observed, one for the ^{1}H signal at δ 21.11, giving a ^{13}C cross-peak at δ −7, and the other for the trace signal δ 33.71 (assigned to the fac isomer) resulting in a ^{13}C cross-peak at δ −52. Cross-peaks for the remaining two Me groups (δ 41.03 and 43.17) are likely to be shifted too far upfield in the ^{13}C NMR spectrum, beyond δ −75, to be detected in this experiment. Additional signals in the ^{1}H NMR spectrum between δ 0 to 5 result from very slow decomposition of the in situ sample because the acquisition of the HMQC spectrum took several hours; the decomposition products, present in trace amounts, are likely to be diamagnetic because the NMR signals are sharp compared to those of paramagnetic **1a**. The ^{13}C signals for these decomposition products are not observed, but cross-peaks are seen between δ 0 to 40 with the ^{13}C NMR spectrum. Only a signal (δ 54) for CD_2Cl_2 is observed in the ^{13}C NMR spectrum for **1a** after 12 h; however, a partial spectrum can be generated from the cross-peaks of the ^{1}H-^{13}C HMQC experiment, producing a spectrum that contains signals for those C atoms that show correlation with signals in the ^{1}H NMR spectrum (Figure 5). The large upfield-shifted resonances for the Me groups (at δ −52 and those not seen below δ −75, compared to values of +20 to +30 within diamagnetic species[10]) in the ^{13}C NMR spectrum are worth noting.

The ^{1}H COSY spectrum of Ru(etma)$_3$ (**1b**) in CD_2Cl_2 (Figure 6) shows three resonance coupling pairs at δ −4.91 *H*(5), 4.86 *H*(6); −0.79 *H*(5), 1.20 *H*(6); and 9.02 *H*(6), 12.54 *H*(5); each pair was assigned to one set of etma *H*(5)/*H*(6) protons, analogous to the ma *H*(5)/*H*(6) assignments for **1a**. The C*H*$_3$ resonances at δ 2.05, 4.78, and 4.86 are coupled to the resonance pairs at δ 35.32, 40.10; 33.41, 38.80; and 18.88, 21.72, respectively, forming a set of three resonances, one for each Et group (Figure 6c and 6d). Each pair of resonances between δ 18.88 and 40.10 corresponds to two diastereotopic C*H*$_2$ protons, as suggested by the cross-peaks in the ^{1}H COSY spectrum. Similarly, each of the etma C*H*$_2$ protons in RuCl(mes) (etma) was observed as a doublet of quartets, by coupling to the other C*H*$_2$ proton and to the adjacent Me group.[3] The ^{1}H NMR data for **1b** show three inequivalent etma ligands, again consistent with a mer geometry. Weak resonances at δ 28.05 and 30.79 for another C*H*$_2$ group give evidence for a small amount of the fac isomer in solution. The C*H*$_2$ resonances for **1b** are shifted downfield similar to the C*H*$_3$ resonances of **1a** because both groups reside in an analogous structural position, adjacent to the C(2) pyridonato ring carbon (see Chart 1). The C*H*$_3$

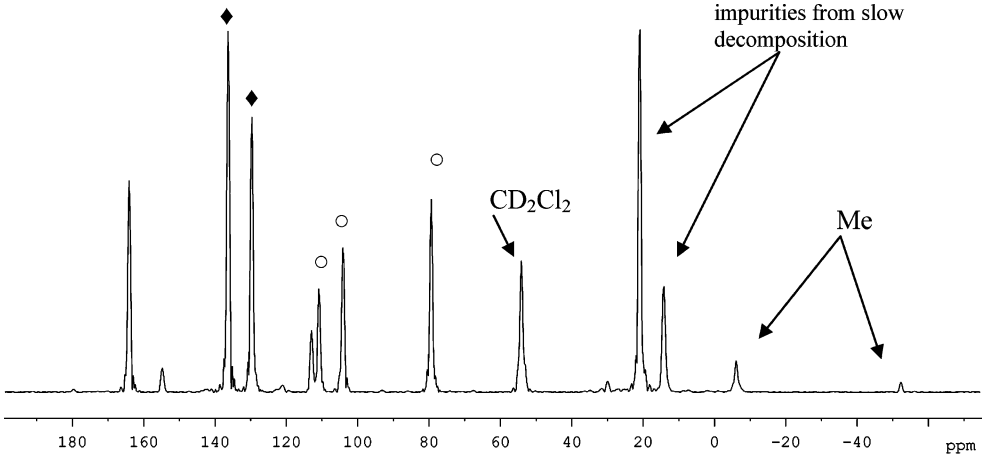

Figure 5. Partial ^{13}C NMR spectrum of **1a** (300 MHz, CD_2Cl_2), generated as a positive projection of the *y* axis from the ^{1}H-^{13}C HMQC spectrum of **1a**. Only C atoms with attached protons giving rise to cross-peaks in the 2D spectrum are observed (○ denotes carbons attached to *H*(6) protons and ♦ denotes those attached to *H*(5) protons).

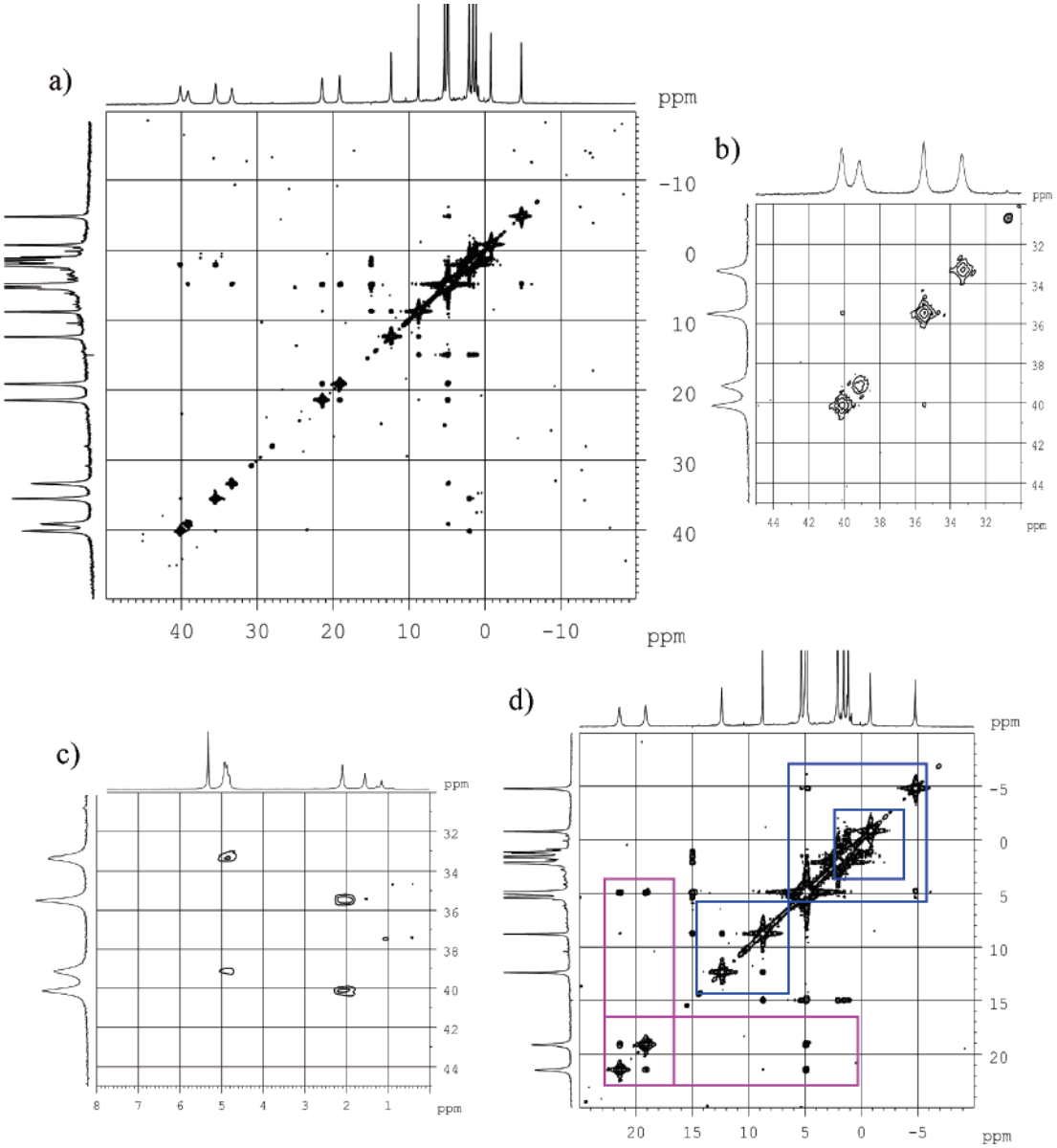

Figure 6. ^{1}H-^{1}H COSY spectrum of **1b** (300 MHz, CD_2Cl_2) showing (a) the complete spectrum, (b) an expansion showing the correlation between the CH_2 protons shifted downfield for two of the ligands, (c) an expansion showing the correlation between the CH_2 and Me protons for the same two CH_2 groups shown in b, and (d) an expansion showing the *H*(5) and *H*(6) correlations for all three ligands (square boxes) as well as the CH_2/Me and CH_2/CH_2 correlations for the third ligand not observed in b or c (rectangular boxes).

protons of **1b** experience only relatively small chemical shifts from that of free etma as the unpaired electron spin density is not effectively transmitted through the sp^3 carbon of the C*H*$_2$ group.[19]

Complex Ru(pyd)$_3$ (**2a**) was synthesized by refluxing a suspension of $RuCl_3 \cdot 3H_2O$, NaOMe, and H(pyd) in EtOH, with workup steps including elution through a silica gel column and reprecipitation with CH_2Cl_2/hexanes. The ^{1}H COSY spectrum of **2a** in CD_2Cl_2 (Figure S1) shows four resonance coupling pairs at δ −4.26 *H*(5), 0.27 *H*(6); −1.54 *H*(5), −1.13 *H*(6); 6.03 *H*(6), 8.59 *H*(5); and 2.89 *H*(5), 7.37 *H*(6), where each of the first three pairs is assigned to one set of *mer*-*H*(5)/*H*(6) protons and the last pair to *fac*-*H*(5)/*H*(6) protons of the pyd ligands. The resonances at δ 5.71, 7.00, 7.89 (*mer*-NC*H*$_3$), and 10.44 (*fac*-NC*H*$_3$) and those at δ 22.71, 27.80, 30.39 (*mer*-C*H*$_3$), and 22.86 (*fac*-C*H*$_3$) are assigned as shown to the six Me resonances for the *mer*-pyd species and two for the *fac*-pyd isomer. The ratio of mer and fac isomers varied somewhat within repeated syntheses, allowing the resonances to be assigned to the proper isomer; the ratio of mer to fac isomers, derived from peak intensities, was typically ~ 3. Trace resonances of free pyd are observed at δ 2.30 (s, C*H*$_3$), 3.45 (s, NC*H*$_3$), 6.25 (d, *H*(5)), and 7.13 (d, *H*(6)), presumably resulting from the dissociation of pyd from the complex. These trace resonances are also observed in D_2O, but conductivity data imply that **2a** is essentially nonconducting in H_2O (see below). The peak intensities of free (diamagnetic) pyd again cannot be compared with those of pyd coordinated at the paramagnetic center.

Some NMR data are available for related complexes of the type Ru(O−O′)$_3$ (e.g. for β-diketonate[20] and tropolonate[21]

species), but we have been unable to find any studies reporting 2D NMR methods and such detailed assignments for paramagnetic $Ru(O-O')_3$ complexes.

The IR $\nu_{C=O}/\nu_{C=C}$ values for **1a** and **1b** are in the 1600−1550 cm^{-1} region, ∼50 cm^{-1} below those of free maltol.[1] The pyd $\nu_{C=O}/\nu_{ring}$ values for **2a** (1600, 1542, and 1498 cm^{-1}) are similar to those reported for RuCl(*p*-cymene) (pyd)[16] and are ∼45 cm^{-1} below those reported for free H(pyd).[22] The Λ_M values of 2 and 5 Ω^{-1} cm^2 mol^{-1} for **1a** and **1b** in CH_2Cl_2, respectively, are consistent with their nonelectrolyte formulation, while corresponding values of 25 and 36 in H_2O suggest that some ma/etma is dissociating from the complexes in aqueous solution, and indeed more complex ^1H NMR data are seen in D_2O. In contrast, **2a** behaves a nonelectrolyte in both CH_2Cl_2 and H_2O.

The reduction potentials ($E_{1/2}$ from a quasi-reversible wave) of **1a** and **1b** in MeCN are essentially identical: −1.13, −1.14 ($Ru^{III/II}$), and 0.52 ($Ru^{IV/III}$) V vs SCE. These values differ significantly from those reported[1] (and reproduced here) for **1a** in CH_2Cl_2 (−1.27 and 0.48 V vs SCE); the differences presumably result from solvent effects.[23] The corresponding potentials for **2a** in CH_2Cl_2 are ∼35−50 mV lower than for **1a**/**1b**, showing that the NMe moiety of pyd is a better electron donor into the ring system than is the O atom of ma or etma (see Chart 1), thereby stabilizing Ru(III) relative to Ru(II). On the basis of literature data for some Ru-oxo-tetraaza ligand systems in acetonitrile,[24] the potential noted at 1.18 V vs SCE is tentatively assigned to a $Ru^{V/IV}$ couple.

The MTT assay reveals that the IC_{50} value for **1b** (90 ± 5 μM) is lower than that for **1a** (140 ± 5 μM), and the AA analysis for **1b** and **1a** (42 ± 5, and 15 ± 5 ng/10^6 cells, respectively) shows that **1b** is taken up into the cell more readily than **1a**; this suggests that the lower IC_{50} may result from more complex being present in the cell, rather than from an increase in specific activity of the complex inside the cell. The IC_{50} values may be compared to that of cisplatin, 30 ± 5 μM, measured under identical experimental conditions. Of note, we have measured IC_{50} values in the 200−400 μM range for Ru(II) complexes of the type Ru(pyronato)-L_2 (L = a sulfoxide, see Introduction), and again, the values for the etma species are lower than those for the corresponding ma complexes.[7] It is worth noting that complexes **1a** and **1b** have been listed in a pharmaceutical patent concerning activity against diseases related to overproduction of species such as NO[25] (the nature of **1a** and **1b** present in the phosphate-buffered saline solutions is, of course, unknown).

Acknowledgment. We thank Ms. Liane Darge and Ms. Marietta Austria for the 2D NMR experiments, Dr. Nick Burlinson for discussions on NMR, and the Natural Sciences and Engineering Research Council of Canada for financial support.

Supporting Information Available: X-ray crystallographic data for the structure of **1a** in CIF format and Figure S1 (the ^1H COSY NMR spectrum of **2a**). This material is available free of charge via the Internet at http://pubs.acs.org.

IC050034D

(19) Eaton, D. R.; Josey, A. D.; Benson, R. E.; Phillips, W. D.; Cairns, T. L. *J. Am. Chem. Soc.* **1962**, *84*, 4100.
(20) Baird, I. R.; Rettig, S. J.; James, B. R.; Skov, K. A. *Can. J. Chem.* **1999**, *77*, 1821 and references therein.
(21) Eaton, S. S.; Eaton, G. R.; Holm, R. H.; Muertterties, E. L. *J. Am. Chem. Soc.* **1973**, *95*, 1116.
(22) Nelson, W. O.; Karpishin, T. B.; Rettig, S. J.; Orvig, C. *Can. J. Chem.* **1988**, *66*, 123.
(23) Bard, A. J.; Faulkner, L. R. *Electrochemical Methods: Fundamentals and Applications*; John Wiley & Sons: New York, 1980.
(24) Wong, K.; Che, C.; Anson, F. C. *Inorg. Chem.* **1987**, *26*, 737.
(25) Simon, F.; Abrams, M. J.; Bridger, G.; Skerlj, R.; Baird, I.; Cameron, B. R. World Patent PCT WO 0056743, 2000.